

Progress in fabrication processing of thin film transistors

Kazuya Yoshioka^{a,*}, Toshiyuki Sameshima^a, Naoki Sano^b

^a Faculty of Engineering, Tokyo University of Agriculture and Technology, 2-24-16 Naka-cho Koganei, Tokyo 184-8588, Japan

^b Hightec Systems Corporation, 3-19-5 Shin-Yokohama, Kohoku-ku, Yokohama, Kanagawa 222-0033, Japan

Available online 26 November 2007

The review of this paper was arranged by Guglielmo Fortunato

Abstract

This paper first discusses laser crystallization of silicon (Si) films with a carbon optical absorption layer, which makes it possible to use an infrared laser light. Then we discuss heat treatment with high-pressure H₂O vapor for defect reduction of laser crystallized Si films and their interface for fabrication of high performance Si thin film transistors (TFTs). Finally, we present a method of transfer process of electrical circuits from original glass substrates to foreign plastic films, developed with GeO₂ removing layer.

© 2007 Elsevier Ltd. All rights reserved.

Keywords: CW laser; Carbon heat source; Defect reduction; Transfer technology; High-rate etching

1. Introduction

Low-temperature fabrication of poly-Si TFTs is now applied to flat display panels [1]. Many important research works have been done on low-temperature fabrication processing of poly-Si TFTs over the past two decades [2–6]. Many researches have been focusing on large grain growth by laser annealing to develop cost-effective poly-Si TFTs with high-performances.

As another research trend, there have been approaches on fabricating poly-Si TFTs on flexible substrates. Especially, transfer technology is expected as one of the promising approaches toward the formation of flexible devices.

This paper describes the authors' recent approaches related to the above topics, laser crystallization and transfer technology for poly-Si TFTs fabrication. Besides, we introduce defect reduction using high-pressure H₂O vapor heat treatment for fabrication of a high-performance TFT.

2. Laser crystallization

Pulsed laser annealing was initially developed for surface modification of bulk semiconductor substrates for 1980s [7–9]. Its application to crystallization of thin films formed on foreign substrates has been simultaneously developed in the same time [2,10]. Many works on pulsed laser crystallization have resulted in application of TFT production to flat panel displays [3,11,12]. High mobility and low threshold voltage is achievable using laser crystallization. Larger grain size reduces a grain boundary number and results in improving TFT performance. Researches on pulsed laser crystallization are currently focused on lateral grain growth. There have been a lot of methods for the lateral grain growth, including substrate heating (~400 °C) [13], double pulse irradiation [14,15], Phase-Modulated Excimer Laser Annealing [16,17], and sample-structural consideration [18,19]. Crystallization of Si films by CW laser is also a promising approach for cost reduction. A very stable, high-power-diode-pumped solid state CW laser (Nd:YVO₄) [20] has been recently developed. It has improved technologies for control of crystalline nucleation and crystallization in the lateral direction.

* Corresponding author. Tel./fax: +81 42 388 7436.

E-mail address: yoshioka@cc.tuat.ac.jp (K. Yoshioka).

Moreover, the authors have also developed a crystallization method of Si films using carbon films as a heating source layer. The method allows us to crystallize Si films with high efficiency for laser in the infrared range as well as the ultraviolet range [21]. We believe that this topic has a possibility of establishment of the cost-effective crystallization processing.

2.1. Si crystallization using a diamond-like-carbon heat source layer by XeCl excimer laser irradiation

We now report about the crystallization with the optical absorption layer. While the high absorption coefficient of Si films, $\sim 10^6 \text{ cm}^{-1}$ at 308 nm, is advantageous to their localized heating with pulsed XeCl laser, the reflection loss of the Si films, $\sim 60\%$ at 308 nm, is a serious problem. Laser crystallization of Si films would be carried out with a less energy irradiation if an excellent heating source layer with a high optical absorbance and high heat resistance is used on the Si films. We discuss rapid thermal crystallization of silicon films with a heating layer of diamond-like-carbon (DLC) films. The previous research revealed that DLC films had low refractive indices from 1.3 to 1.9 and high extinction coefficients from 0.8 to 0.9 for wavelengths from 250 to 1100 nm [22]. These properties resulted in optical absorbance higher than 0.7 for 200 nm-thick DLC films at wavelengths shorter than 1000 nm.

Fig. 1 shows Raman scattering spectra of silicon films for 100 nm-DLC/5 nm-SiO₂/25 nm-Si/quartz (a) and 25 nm-Si/quartz (b) when the samples were irradiated with the XeCl excimer laser [22]. Note the DLC films were formed by a plasma-sputtering method using a carbon target. The Raman scattering measurement was carried out

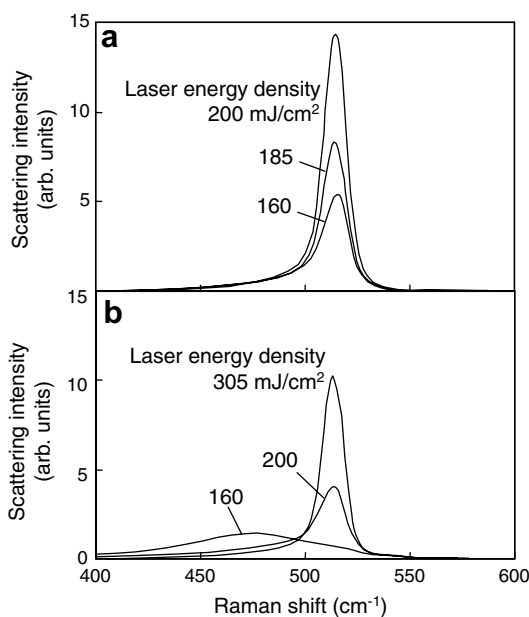


Fig. 1. Raman scattering spectra of silicon films 100 nm-DLC/5 nm-SiO₂/25 nm-Si/quartz (a) and 25 nm-Si/quartz (b) when the samples were irradiated with XeCl excimer laser with different energy densities.

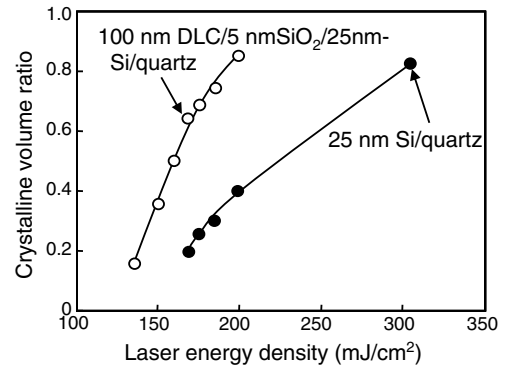


Fig. 2. Crystalline volume ratio of poly-Si obtained by analyzing of optical reflectivity spectra in the ultraviolet region, as a function of laser energy density.

after removing the DLC films by oxygen plasma etching after laser irradiation. High and sharp phonon bands of Si were observed for the laser-crystallized Si films at laser energy densities from 160 to 200 mJ/cm² in the case of the 100 nm-DLC/5 nm-SiO₂/25 nm-Si/quartz structure. On the other hand, there was no crystalline phonon band for laser irradiation at 160 mJ/cm² for 25 nm-Si/quartz due to laser energies just below the crystallization threshold for the Si/quartz structure.

The intensity of the crystalline phonon band was very low with 200 mJ/cm² laser irradiation for the Si/quartz structure. An energy density of 305 mJ/cm² was necessary in order to form crystalline Si with a phonon intensity comparable to that of 100 nm-DLC/5 nm-SiO₂/25 nm-Si/quartz formed at 200 mJ/cm².

Fig. 2 shows the crystalline volume ratio, obtained by analyzing optical reflectivity spectra in the ultraviolet region, as a function of laser energy density. The detailed analytical method to determine the crystallization volume ratio is described in Ref. [22]. Crystallization was observed with laser energy above 135 mJ/cm² for the 100 nm-DLC/5 nm-SiO₂/25 nm-Si/quartz, although the crystallization threshold was 170 mJ/cm² for the 25 nm-Si/quartz. The crystalline volume ratio of the silicon films was 0.85 at 200 mJ/cm² for the 100 nm-DLC/5 nm-SiO₂/25 nm-Si/quartz, while it was only 0.4 in the case of the 25 nm-Si/quartz. These results obviously show that the 25 nm-thick Si films were well crystallized even at a laser energy density of as low as 200 mJ/cm² when the DLC heating layer was used.

2.2. Si crystallization using a carbon particle heat source layer by continuous-wave infrared laser irradiation

We recently proposed to use a cheap infrared continuous-wave (CW) laser diode with a cheap optical absorption layer to crystallize Si films at a low cost. For the purpose, we use a carbon particle layer formed by the spin coating method instead of using DLC films formed by sputtering method. Carbon particles dispersed in water with a concen-

tration of 15 wt.% were then coated on the silicon films using a spinner at a rotation speed of 5000 rpm. The mean diameter of the carbon particles was about 200 nm. We investigated crystallization conditions of the silicon films using a carbon/50 nm-a-Si/quartz structure.

Fig. 3 shows the experimental setup for laser irradiation with the beam scanning mechanisms. Laser irradiation normal onto the carbon layer with underlying silicon films was carried out in the air by a fiber coupled CW laser diode with a wavelength of 940 nm and a maximum power of 20 W [21]. The diameter of the core and the numerical aperture (NA) of the fiber was 400 μm and 0.22, respectively. The diverged beam was focused on the surface of samples of carbon/Si/glass by a combination of six aspherical lenses for 1:1 image formation on samples at room temperature. The power distribution of the beam is Gaussian one with peak intensity of 14–70 kW/cm^2 . The full width at half maximum (FWHM) was set at 180 μm . Samples were mounted on an X–Y moving stage, which was moved at a constant scanning speed of 100 cm/s in the Y direction keeping the size, shape and the intensity of the laser spot. We set the constant period of 10–50 μm in the X direction of scanning lines.

Fig. 4 shows Raman scattering spectrum of the silicon film irradiated at a laser power of 20 W. A high scattering intensity and a sharp crystalline phonon band were observed. There was no residual amorphous band. As a laser with a beam diameter of 1 μm had been used for the Raman scattering measurement, we predicted quite a large grain with a few microns had been obtained. Fig. 5 shows the crystalline volume ratio, obtained from the peak analyses of transverse optical phonon peak of crystalline, microcrystalline and amorphous Si around the wavenumbers of 520, 500 and 480 cm^{-1} , respectively, as a function of laser power. Crystallization was observed at laser pow-

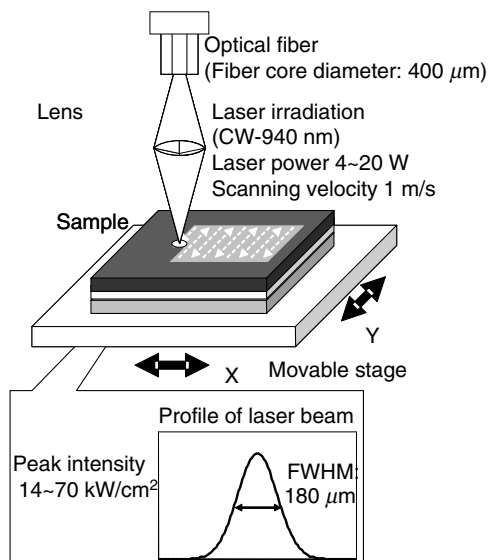


Fig. 3. Apparatus for crystallizing Si films with carbon optical absorption layer by an infrared continuous-wave laser irradiation.

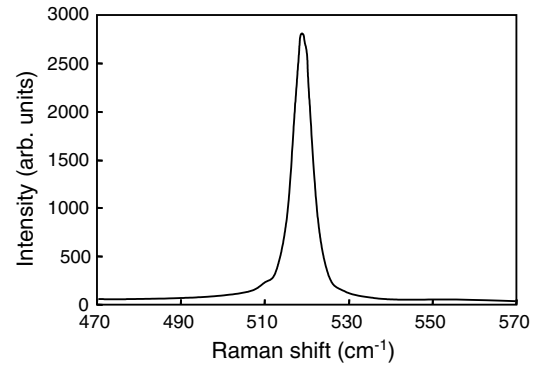


Fig. 4. Raman scattering spectra of silicon films for carbon/50 nm-Si/quartz when the samples were irradiated with a 940 nm CW laser at a laser power of 20 W and the scan speed of 100 cm/s .

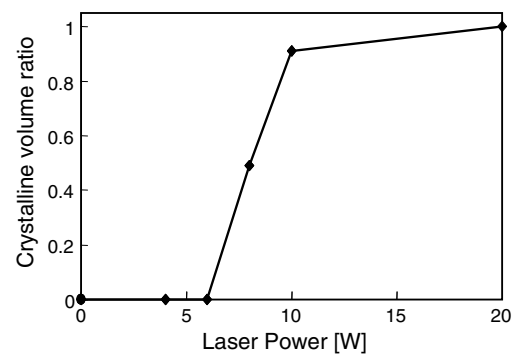


Fig. 5. Crystalline volume ratio of poly-Si, obtained from the peak analyses of transverse optical phonon peak of crystalline, microcrystalline and amorphous silicon around the wavenumbers of 520, 500 and 480 cm^{-1} , as a function of laser power.

ers above 6 W and the crystalline volume ratio increased with the laser power from 6 to 20 W. A very high crystalline volume ratio of 1.0 was obtained at a laser power of 20 W. This suggests that the carbon films effectively absorbed the 940 nm infrared laser light and were heated to high temperature to crystallize a Si film.

3. Defect reduction

Reduction of defects by post-laser-annealing is important for obtaining good TFT characteristics. Several techniques have been developed including hydrogen plasma treatment and oxygen plasma treatment. We here discuss heat treatment with high-pressure H_2O vapor developed by the authors which is also effective for defect reduction of polycrystalline silicon films [23,24].

Fig. 6 shows the electrical conductivity of a $7.4 \times 10^{17} \text{ cm}^{-3}$ phosphorus-doped 50 nm-thick Si films crystallized at $400 \text{ mJ}/\text{cm}^2$ as a function of heating temperature with $1.3 \times 10^6 \text{ Pa}$ H_2O vapor for 1 h and 3 h [23]. The electrical conductivity was increased from $1.3 \times 10^{-5} \text{ S}/\text{cm}$ (initial) to as high as 2 S/cm by annealing with the 270 $^\circ\text{C}$ H_2O vapor for 3 h. The figure also shows change in the electrical conductivity as a function of heating temperature for 3 h in dry

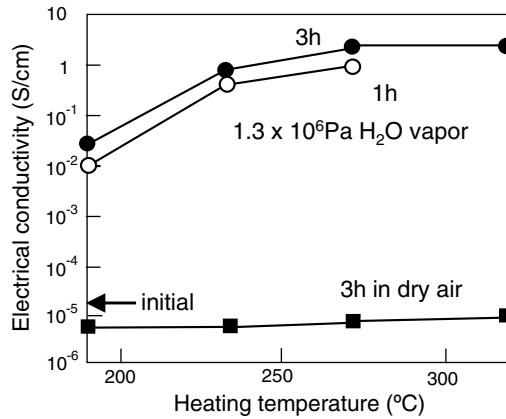


Fig. 6. Changes in the electrical conductivity as a function of heating temperature with 1.25 GPa H₂O for 1 h and 3 h, respectively, and as a function heating temperature in dry air for $7.4 \times 10^{17} \text{ cm}^{-3}$ phosphorus-doped 50 nm-thick Si films laser-crystallized at 400 mJ/cm².

air. No marked increase in the electrical conductivity was observed in the case of the heat treatment in the dry air. These results clearly show that the electrical properties of the laser crystallized Si films were markedly changed by heat treatment with high-pressure H₂O vapor at 190–300 °C, although the simple heating in dry atmosphere yielded no appreciable change for the entire temperature range considered.

Fig. 7 shows changes in the electrical conductivity as a reciprocal function of temperature for initial silicon films laser-crystallized at 400 mJ/cm² and room temperature, and films annealed with H₂O vapor at 190 and 270 °C for 1 h and 3 h, respectively [23]. The electrical conductivity of the initial crystallized films (with activation energy of 0.55 eV) increased as the temperature increased. On the other hand, the electrical conductivity increased and the activation energy decreased after high-pressure H₂O vapor

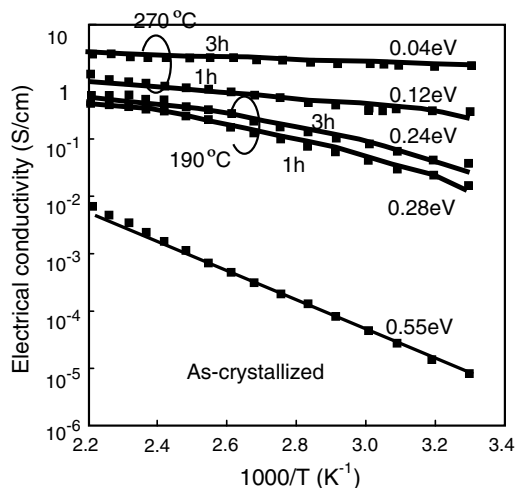


Fig. 7. Changes in the electrical conductivity as a reciprocal function of temperature for $7.4 \times 10^{17} \text{ cm}^{-3}$ phosphorus-doped 50 nm-thick Si films laser-crystallized at 400 mJ/cm² and films annealed with H₂O vapor at 190 and 270 °C for 1 h and 3 h, respectively.

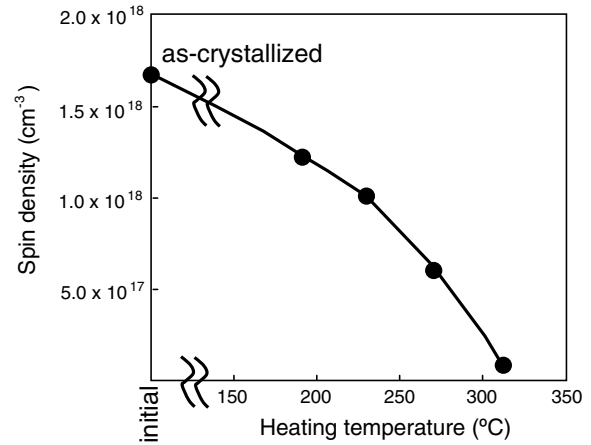


Fig. 8. Spin density of undoped 50 nm-thick silicon films laser crystallized at 400 mJ/cm² as a function of heating temperature. Heat treatment was carried out with $1.3 \times 10^6 \text{ Pa H}_2\text{O}$ vapor for 3 h.

treatment. This result means that the free carrier density increased after the treatment.

In order to investigate the effect of heat treatment with high-pressure H₂O vapor, electron spin resonance (ESR) measurements were conducted to measure the spin density of undoped, laser crystallized 400 mJ/cm² silicon films before and after the heat treatment. Fig. 8 shows the spin density as a function of heating temperature for heat treatment at $1.3 \times 10^6 \text{ Pa}$ for 3 h [23]. The initial films had a high spin density of $1.6 \times 10^{18} \text{ cm}^{-3}$ caused by dangling bonds localized at grain boundaries [23]. The spin density was reduced to $1.2 \times 10^{17} \text{ cm}^{-3}$ by heat treatment at 310 °C. H₂O molecules at defect sites would be chemically dissociated with the help of heating energy. The dangling bonds of silicon atoms were probably eliminated through the formation of Si–O, Si–OH or Si–H bonds.

4. Transfer technology for poly-Si TFTs

Transfer technology can be promising to form thin-film electrical circuits on inexpensive flexible substrates. The laser induced forward transfer of hydrogenated amorphous silicon (a-Si:H) films was initially reported in 1994 [25]. After that, the laser-induced transfer with a-Si:H layers has been developed to a practical level [26]. To date, several transfer methods have been proposed [25–31]. The authors have also proposed a transfer method by the wet etching of a GeO_x removing layer [31]. We now present some significant results of rapid removal of the GeO_x layers and successful transferring thin film layers to plastic films.

GeO_x films were formed by 13.56 MHz plasma sputtering with a germanium target at a RF power of 1 kW in mixed gases of argon (Ar) and oxygen (O₂). The GeO_x films formed at 40 sccm Ar and 20 sccm O₂ flow rates were found to have almost a constant refractive index of 1.6 at visible wavelengths by the numerical analysis of their transmissivity spectra. The optical absorption peak in infrared region was observed on the GeO_x films at a wavenumber of 870 cm⁻¹, resulting from Ge–O bonding. Rutherford

backscattering spectrometry revealed a component ratio between Ge and O was 1:2 for the GeO_x films formed at 40 sccm Ar and 20 sccm O_2 flow rates.

The GeO_2 films are soluble in water. The etching rate of the GeO_2 films in H_2O was investigated as a function of H_2O temperature, using an optical method. A 3 μm -thick- $\text{GeO}_2/100$ nm-a-Si/quartz structural sample was dipped in the H_2O so as to be irradiated normally to its surface with a 632 nm He–Ne laser beam. The etching time was determined as the period when the intensity of the laser beam transmitting the sample had been changed, because the transmissivity of the sample change with the thickness of the GeO_2 film due to an optical interference effect. Fig. 9 shows the etching rate of the 3 μm -thick GeO_2 films in H_2O as functions of H_2O temperature [33]. The etching rate increases with the H_2O temperature. Higher temperature probably promotes chemical reaction of GeO_2 with H_2O .

In order to examine transfer of thin films, a 1 μm -thick GeO_2 removing layer was formed on a glass substrate. Then, a 200 nm-thick amorphous silicon layer was formed on the GeO_2 layer by sputtering. A plastic substrate was attached to the device layer using an adhesive of silicone. The plastic/silicone/a-Si:H/ GeO_2 /glass structural sample was dipped in hot H_2O until the GeO_2 layer was completely dissolved out and the plastic/silicone/a-Si:H was completely separated from the glass substrate. Although a high lateral etching rate of 1.8 $\mu\text{m}/\text{s}$ was obtained for the GeO_2 film at 80 °C in H_2O , it took about 8 h to complete the transfer process for a 4 in. sized sample because of simple lateral etching of GeO_2 .

We developed a quick transfer process using a thermo-setting-type epoxy adhesive as the adhesive layer and applying thermal stress. A layered structure of plastic/270 μm -epoxy/50 nm-a-Si/200 nm- $\text{SiO}_2/1$ μm - GeO_2 /quartz was formed at a diameter of 4 in. [33]. The sample was immersed in H_2O 80 °C for 90 min to dissolve out the GeO_2 layer at edge region by 4–6 mm. Then the sample was cooled by picking it out of the 80 °C H_2O in the ambient air. The residual GeO_2 layer quickly and completely dissolved out in 2 min. after picking it out to the ambient air. This means a rapid lateral etching of GeO_2 was achieved at 370 $\mu\text{m}/\text{s}$, which was 2 orders of magnitude

higher than the etching rate before the cooling. The 50 nm-a-Si/200 nm- SiO_2 layers were consequently transferred to the 4 in. plastic substrate with few visible cracks and wrinkles as shown in Fig. 10. Any additional cracks and wrinkles were not observed even with an optical microscope with 50-fold magnification.

We interpret the following mechanism for the rapid increase in the lateral etching rate of the GeO_2 . The sample was slight bending inward at room temperature because of the thermal stress between the epoxy layer and the quartz substrate since the epoxy adhesive was cured at 120 °C for 30 min. The epoxy has the thermal expansion coefficient two orders of magnitude higher than the quartz substrate. The normal stress is dominant at the sample edge between the quartz and epoxy layers [32]. When the sample was cooled to the ambient temperature after treatment in 80 °C H_2O , the stress concentrated at the edge of the residual GeO_2 layer. The stress peeled the epoxy layers from the quartz substrate at the edge region because the GeO_2 became weak owing to bond breaking of Ge–O by hot water attack. This phenomenon promoted water penetration into the inner region of the GeO_2 layer by the capillary phenomenon. GeO_2 at edge region is further dissociated by the water. Consequently, the stress continued to peel the epoxy layers from the quartz substrate.

This transfer technique was also applied to transferring a poly-Si TFT array with an area of 20 cm^2 [34]. The n-type poly-Si TFTs with a channel width and length of 1 mm and 0.5 mm were fabricated using existing TFT processes on the top layer of 200 nm- $\text{SiO}_2/1$ μm - GeO_2 /quartz samples. For a plastic/silicone/epoxy/poly-Si-TFTs/200 nm- $\text{SiO}_2/1$ μm - GeO_2 /quartz sample, transfer demonstration was carried out. Most of the TFTs were successfully transferred in 30 min without damages killing TFT operation as seen from the microphotographs of Fig. 11. Fig. 12 shows the transfer curve for one of the fabricated TFTs before and after the transfer process. The drain current fairly increased at gate voltage of 10–15 V after the transfer process. The reason is now under investigation. These experimental results suggest the concept of the present transfer process is valid.

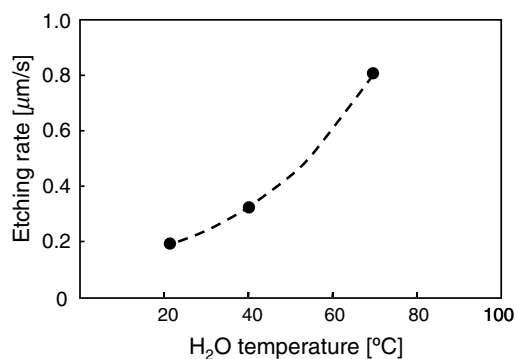


Fig. 9. Etching rates of 3 μm -thick GeO_2 films in H_2O as functions of H_2O temperature.

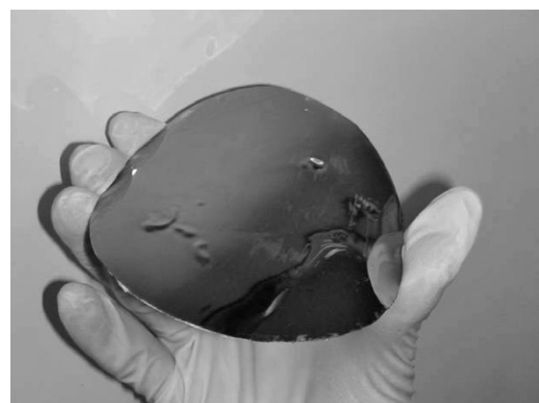


Fig. 10. An a-Si film transferred onto the 4 in. plastic substrate.

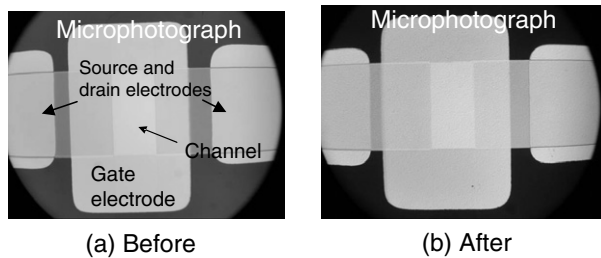


Fig. 11. Microphotographs of a single TFT before and after the transfer process.

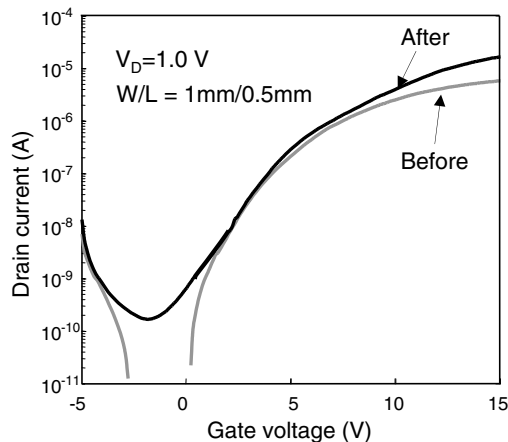


Fig. 12. Transfer curves for a poly-Si TFT before and after the transfer process.

5. Summary

The authors' recent activities were presented on the fabrication processing for TFTs. We discussed crystallization of Si films with a carbon heating layer by pulsed lasers and an infrared CW laser, respectively. By the use of the carbon heating layer, Si films were well crystallized at less energy in the case of XeCl excimer laser irradiation. The study also showed that the application of an infrared CW laser could be used to obtain crystallized Si films with a very high crystalline volume ratio of 1.0. High-pressure H₂O vapor treatment was shown to be effective method for defect reduction of as-crystallized poly-Si films from experimental data.

We investigated a method to transfer thin-film circuits to foreign substrates using a GeO₂ removing layer. The GeO₂ removing layer could be quickly removed by applying thermal stress after dissolving near edge region of the GeO₂ layer for a transfer sample with a relatively-hard epoxy resin layer on the thin-film-device layer. A TFT array with an area of 20 cm² was transferred with few damages.

Acknowledgements

The authors thanks to Drs. K. Takechi and N. Andoh for their support.

References

- [1] Uchikoga S, Ibaraki N. Low temperature poly-Si TFT-LCD by excimer laser anneal. *Thin Solid Films* 2001;383:19.
- [2] Sameshima T, Usui S, Sekiya M. *IEEE Electron Device Lett* 1986;7:276.
- [3] Sera K, Okumura F, Uchida H, Itoh S, Kaneko S, Hotta K. *IEEE Trans Electron Device* 1989;36:2868.
- [4] Serikawa T, Shirai S, Okamoto A, Suyama S. *Jpn J Appl Phys* 1989;28:L1871.
- [5] Kohno A, Sameshima T, Sano N, Sekiya M, Hara M. *IEEE Trans Electron Device* 1995;42:251.
- [6] Chen Z, Pang SK, Yasukake K, Rohatigi AJ. *Appl Phys* 74, 2856.
- [7] Wood RF, Giles CE. *Phys Rev B* 1981;23:2923.
- [8] Lowndes DH, Kirkpatrick Jr GH, Pennycook SJ, Withrow SP, Mashburn DN. *Appl Phys Lett* 1986;48:1389.
- [9] Deutsch TF, Fan JCC, Turner CW, Chapman RL, Ehrlich DJ, Osgood Jr RM. Efficient Si solar cells by laser photochemical doping. *Appl. Phys. Lett.* 1981;38:144.
- [10] Sameshima T, Usui S, Sekiya M. *IEEE Electron Device Lett* 1986;EDL-7:276.
- [11] Kuriyama H, Kuwahara T, Ishida S, Nohda T, Sano K, Iwata H, et al. *Jpn J Appl Phys* 1992;31:4550.
- [12] Mathé EL, Maillou JG, Naudon A, Fogarassy E, Elliq M, De Unamuro S. *Appl Surf Sci* 1989;43:142.
- [13] Kuriyama H, Nohda T, Aya Y, Kuwahara T, Wakisaka K, Kiyama S. *Jpn J Appl Phys* 1992;33:5657.
- [14] Ishihara R, Matsumura M. *Electron Lett* 1995;30:1956.
- [15] Jumonji M. *Jpn J Appl Phys* 1996;35:6592.
- [16] Chang-Ho OH, Ozawa M, Matsumura M. *Jpn J Appl Phys* 1998;37:L492.
- [17] Taniguchi, Matsumura M, Jyumonji M, Ogawa H, Hiramatsu M. *J Electrochem Soc* 2006;153:G67.
- [18] Kim CH, Song IH, Nam WJ, Han MK. *IEEE Electron Device Lett.* 23 2002:325.
- [19] Van-der-Wilt PCh, van Dijk BD, Bertens GJ, Ishihara R, Mater Res Soc Symp Proc, 685E, D5.20, 2001.
- [20] Hara A, Takeuchi F, Takei M, Suga K, Yoshino K, Chida M, et al. *Jpn J Appl Phys* 2002;37:L5.
- [21] Sano N, Maki M, Andoh N, Sameshima T. In: *Proceeding of International Workshop on Active-Matrix Flatpanel Displays and Devices '06*, 2006, p. 329.
- [22] Sameshima T, Andoh N. *Jpn J Appl Phys* 2005;44:7305.
- [23] Asada K, Sakamoto K, Watanabe T, Sameshima T, Higashi S. *Jpn J Appl Phys* 2000;39:3883–7.
- [24] Sameshima T, Satoh M, Sakamoto K, Ozaki K, Saitoh K. *Jpn J Appl Phys* 1998;37:L1030.
- [25] Sameshima T. *Appl Surf Sci* 1996;96–98:352.
- [26] Inoue S, Utsunomiya S, Saeki T, Shimoda T. *IEEE Trans Electron Device* 2002;49:1353.
- [27] Takayama T, Ohno Y, Goto Y, Machida A, Fujita M, Maruyama J, Kato K, Koyama J, Yamazaki S. 2004 symposium on VLSI Technology Digest of Technical Papers, 2004; p. 230–1.
- [28] Asano A, Kinoshita T. *SID Symposium Digest* 2002;33:1196.
- [29] Hioki T, Akiyama M, Nakajima M, Tanaka M, Onozuka Y, Hara Y, Naitoh H, Mori Y. In: *Proceedings of the International Display Workshop 2002*; p. 319–32.
- [30] Takechi K, Eguchi T, Kanoh H, Ito T, Otsuki S. *IEEE Trans Semiconduct Manuf* 2005;18(3):384–9.
- [31] Sameshima T, Yoshioka K, Takechi K. *Jpn J Appl Phys* 2005;44.
- [32] Toyoda M, Komatsu T, Satoh K, Nayama M. *International Institute of Welding Technical Doc.*, 1988; X-1161-88.
- [33] Yoshioka K, Yamamoto M, Sameshima T, Takechi K. In: *Proceedings of ITC'06*, 2006, p. 158.
- [34] Yoshioka K, Sameshima T, Takechi K. In: *Proceedings of International Workshop on Active-Matrix Flatpanel Displays and Devices '06*, 2006, p. 139.